

CrossRef DOI of original article:

Establishment of an Analytical Model for Determining Leakage Surfaces in an External Tooth Spur Gear

Choupo Wankam Gervé¹ and Tchotang Théodore²

¹ University of Yaounde I, Yaounde, Cameroon. National Advanced School of Engineering, Civil and Mechanical Engineering Laboratory

Received: 1 January 1970 Accepted: 1 January 1970 Published: 1 January 1970

Abstract

In gear power transmission systems, the lubricant helps reduce friction, wear of parts in contact, cooling of surfaces, reduction of operating noise, protection of components against corrosion, etc. In spite of that, the lubricant entrapment in the gears inter-tooth space generates substantial energy losses at very high rotational speeds. The best optimization of these energy losses requires the preliminary knowledge of the behavior of leakage surfaces of trapped lubricant during the gears rotation. The aim of this work is to develop a purely analytical model enabling to calculate the exact values of the axial and radial leakage surfaces of the lubricant in the inter-tooth space of external spur gears as well as the volumes of the pockets. From the modeling of the tooth profile and the parametric equations relating to external spur gears, we have developed a purely analytical model of the lubricant leakage surfaces in the inter-tooth space as a function of the angle of rotation. Validation of the model was carried out via a comparative study between our results and those resulting from the work of Abdelilah LASRI and al and Diab Y. and al. Curves from our model and those of the reference articles merge after superposition and the relative differences are less than 10-2. This work is therefore the first step in the calculation of the power lost by the lubricant trapping in the gears inter-tooth. It will be of great importance in minimizing power losses.

Index terms— gear, power transmission, energy losses, trapping, leakage surfaces, pocket volumes, inter-tooth.

1 I. Introduction

Due to their compactness and their ability to transmit high loads at high speeds, gears are widely used in automotive and aerospace applications through speed reducers, power transmissions in wind turbines, etc. In gear drives energy efficiency improving may require reducing power losses. Power losses in gears (gearboxes, reducers, etc.) can be grouped into two categories: power losses depending on the transmitted load (friction at the contact areas between the teeth and friction in the bearings, etc.) and those independent of the transmitted load (losses due to the trapping of the lubricant, the ventilation of the mobiles, etc.). Several researchers have been interested in load-dependent losses and enough models exist. The oil trapping in the inter-tooth space and the ventilation of the spindles are the two main sources of power dissipation in the case of losses independent of the loads. Very few studies and models exist on the loss of power by lubricant trapping and by consequent on the modeling of lubricant leakage surfaces. The vast majority of studies concerning the modeling of lubricant trapping in the inter-tooth space are empirical, numerical, and semi-analytical and based on approximations and estimations.

Using NASA research center test rig, Anderson and al. [2], Krantz [3], Rohn and Handschuh [4] have developed several empirical formulas. Empirical formulations for the particular case of trapping losses in gears are based on the gears geometric parameters and include those of Terekhov [5], Wolfan Mauz [6], Butsch M. [7] and Maurer

3 D) GEOMETRY OF A SPUR GEAR TOOTH

J. [8]. The empirical models developed provided global formulas for the estimation of pressing torque or power loss. It is necessary to point out that these formulas are only valid for external gearing and remain linked to the sensitivity and precision of the equipment used for the tests. Generally they are of very low precision with quite important deviations. As an example we can quote the model of Mauz [6], which indicates an uncertainty between 5 and 15% if the resisting torque is higher than 5 Nm and an uncertainty up to 50% for lower torque values. It is therefore necessary to set up another quite precise model. Many researchers have developed numerical models to understand the behavior of inter-tooth spaces during movement in order to estimate the power lost by trapping. Pechersky and Wittbrodt [9] used an approximation of the tooth profile expression to calculate the leakage surfaces. Diab Y. and al [10][11] have numerically evaluated the radial leakage surfaces (considered here as minimum distances between the tip corner of the gear and the profile) and they obtained the axial leakage surfaces by The first experimental studies on this subject permitted to make a difference between load-dependent and load-independent losses. Devin R. and Hilty B. [1], made experimental investigations of load-independent losses caused by planetary gear sets and conclude that for high speeds (≈ 6000 rpm) the losses independent of the load become the major contributor. These experimental works allowed to develop and validate empirical, numerical and semi-analytical models. numerical integration. Abdelilah Lasri and al [12][13][14] used a numerical approximation to evaluate the radial surfaces (considered here as the minimum distance between the tooth profiles) and they obtained the axial leakage surfaces by numerical integration. David C. Talbot [15] calculates the power lost by trapping in planetary gears by discretizing in time and space the Conservation of Mass, Momentum and Energy equations. The leakage surfaces are obtained by numerical approximation through the surfaces meshing. Seetharaman and Kahraman [16] were inspired by the work of Pechersky and Wittbrodt [9] to establish a semi-analytical formulation for calculating leakage surfaces. However, several approximations are made there, namely a Taylor approximation of order 1 of the involute profile equation, the cancellation of certain portions of the surface, the use of approximate values of certain distances, etc. From the vectors ray approach, Massimo Rundo [17] established an analytical formula for trapped volume in crescent pumps. It is necessary to note that in this approach the length variation of the vector ray for an infinitesimal rotation is neglected. In addition, this formula is limited only to the portion where teeth profiles are in contact. For an efficient contribution to the power losses by the lubricant trapping of as well as the wear of the elements with a view to improve the energy performances in gears transmissions, it is essential to completely lift the veil on the inter-tooth zone during meshing. From the work of Seetharaman and Kahraman [16], we will establish a purely analytical model of the evolution of the radial and axial leakage surfaces as a function of the angle of rotation in a spur gear. This work has as particularity the use of the exact expression of the tooth profile in the calculations and the authenticity of the analytical expressions of the developed surfaces.

This work is divided into three main parts. The first part is devoted to the modeling of the tooth profile and the associated parametric equations. The second part deals with the calculations of the leakage surfaces from the tooth profile equations, with the radial leakage surface being considered as the minimum distance between the tooth profiles. The last part focuses on the results interpretation and the model validation. The model validation consist of a superposition of our results with those of A. Lasri and al [13] and Diab and al [10].

2 II. Material a) Trapping Phenomenon

The lubricant used in gear transmissions to reduce corrosion, friction, cool the elements, etc., is trapped in the inter-tooth space during movement and becomes the seat of energy losses. Lubricant trapping is the jamming of the lubricant in the inter-tooth space during the meshing phase. The fraction of lubricant trapped in the inter-tooth space (in yellow in figure 1) is expelled under pressure radially toward the neighbouring pockets and or axially toward the outside of the gear during this phenomenon. The opposite phenomenon is reproduced during the unmeshing phase.

The geometry of the inter-tooth space relates to the type of tooth (straight, helical, hypoid, etc.) which constitutes the gear's wheels. In the particular case of spur gears, the axial leakage area remains constant over the tooth width. However, in the case of helical gear, the axial leakage area is variable over the tooth width. The radial and axial leakage surfaces vary according to the angle of rotation. The further away from the initial position, the surfaces increase. Here, the initial position is the meeting point between the two pitch circles. The Figure 2 below illustrates the behavior of the leakage surfaces as a function of the angle of rotation (from a) to h). The pinion (driver) is associated to a fixed reference (O_1, θ_1) , (O_1, θ_1) , (O_1, θ_1) , (O_1, θ_1) , which revolves around (O_1, θ_1) , (O_1, θ_1) by an angle θ_1 . Similarly, the gear (driven) is associated to fixed reference (O_2, θ_2) , (O_2, θ_2) , (O_2, θ_2) , (O_2, θ_2) and mobile reference (O_2, θ_2) , (O_2, θ_2) , (O_2, θ_2) , which revolves around (O_2, θ_2) , (O_2, θ_2) by an angle θ_2 . Such as In our calculations, the initial position is the position where the tooth profiles of the driving and driven gears meet at point I (the contact point between the pitch circles). $\theta_2 = (\theta_1 / \theta_2)$ $\theta_1 = (\theta_1 / \theta_2)$ $\theta_1 = (\theta_1 / \theta_2)$ $\theta_1 = (\theta_1 / \theta_2)$ θ_1 .

3 d) Geometry of a Spur Gear Tooth

The tooth shapes of spur gears are relative to the number of teeth. Generally, for a tooth, there will be the involute zone and the circular zone. In a specific interval of the rotation angle, the profiles of the teeth meet,

103 and consequently the radial leakage surfaces remain zero. Figure 5 below is a particular case. On this figure, C1
 104 and C2 are the two contact points of the tooth profiles. The simulation of the equations and the model obtained
 105 was carried out with the MATLAB R2016A application installed in an HP computer, AMD A6-3400 APU HD
 106 Graphics 1.40 GHz; 6 GB of RAM.

107 4 III. Method a) Hypothesis

108 Our study was carried out under the following assumptions:

- 109 -The portion of tooth between the addendum circle and the base circle is in involute.
- 110 -The shape of the tooth portion after the base circle varies depending on the tooth number.
- 111 -Radial distances are minimum distances between adjacent profiles.
- 112 -The direction of rotation of positive angles is the trigonometric direction and, the direction of rotation of
 113 negative angles is the anti-trigonometric direction. -In our calculations, the initial position ($\theta = 0$) is
 114 the position where the two adjacent profiles meet at the common point of the pitch circles. However, for the
 115 presentation and the comparative study of the results, we bring the initial position back to the position where
 116 (O 1 O 2) passes simultaneously through the midpoints of the gear top land and the pinion root.

117 5 b) Calculation Algorithm

118 From the geometric parameters of a gear tooth, the parametric equations of the half tooth profile are established.
 119 The complete gear tooth is obtained by axial symmetry of this half tooth, followed by N-1 successive rotations
 120 of the primary tooth with respect to the axis of the gear and respective angles $2\pi k/N$, $1 \leq k \leq N-1$. Where N is
 121 the number of teeth.

122 From the initial position, the coordinates of the boundary points of the leakage surfaces are calculated as a
 123 function of the rotation angle. From the properties of the involute of a circle, we calculate the radial distances
 124 as a function of the rotation angle and by surface integration, we obtain the radial surfaces. The figure 7 below
 125 is the algorithm that succinctly presents our working methodology.

126 6 1) Tooth tip equation

127 The tooth tip is a fraction of the tip circle (see figure 4). By applying the parametric equation of a circle with
 128 radius r_t (tip radius) centered in the point O_1 , the parametric equation of the half of the gear tooth tip is
 129 given in the coordinate system (o, x, y) by the relation (1) below:

130 With $\theta = \arccos(r_b/r_t)$, $\theta = \arccos(r_b/r_t)$ = mes(θ , θ) and $\theta = \theta$

131 7 2) Equations of the involute portion (AB)

132 By applying the properties of the involute of the circle, the parametric equations of the portion (AB) in the fixed
 133 frame (O,x,y) are given by the relation (2) below:with $0 \leq \theta \leq \arccos(r_b/r_t)$

134 8 3) Equations of the portion between the base circle and the 135 root circle

136 On the figure 6, $\theta = \arccos(r_b/r_t)$ (3)

137 with $\theta = \arccos(r_b/r_t)$ = $\arccos(r_b/r_t)$. By application of the geometric construction properties (see [20])
 138 $\theta = \arccos(2r_b r_p / (r_b^2 + r_p^2))$.

139 In the cas of gears with pressure angle $\alpha = 20^\circ$, when $\theta = \arccos(2r_b r_p / (r_b^2 + r_p^2))$ then
 140 we take $\theta = k * ((\pi/N) - \alpha)$; $0 < k < 1$.

141 In summary, in the portion between the base circle and the root circle 03 possible profiles shapes emerge
 142 depending on the number of teeth:

143 -If $\theta = 0$: The circular portion does not exist. Our tooth will consist only of the involute part and
 144 the tooth top.

145 -If $\theta > 0$: Two possibilities emerge. If $\arccos(2r_b r_p / (r_b^2 + r_p^2)) > \theta$
 146)) $\theta = \arccos(2r_b r_p / (r_b^2 + r_p^2))$: In this case, this portion will consist of two (02) types of profiles, namely the arc of a circle
 147 BD followed by the root circle. If $\arccos(2r_b r_p / (r_b^2 + r_p^2)) < \theta$

148)): In this case, this portion is broken down into segment [BC] and arc of circle CD followed by the part of
 149 the root circle. $x = r_b \cos(\theta)$, $y = r_b \sin(\theta)$ (1) $x = r_b \cos(\theta)$, $y = r_b \sin(\theta)$
 150 $x = r_b \cos(\theta)$, $y = r_b \sin(\theta)$ (2) $x_B = r_b \sin(\theta)$, $y_B = r_b \cos(\theta)$ (4) $x_D = r_p \sin(\theta)$
 151 $y_D = r_p \cos(\theta)$ (5) Year 2022 © 2022 Global Journals

152 Let K be the contact point between the tangent to θ in D and the tangent to the involute in B. Then
 153 the coordinates of K are given by relation (6) In this case, the center of curvature is given by the relation (12)
 154 below:

155 Where $\theta = \arccos(2r_b r_p / (r_b^2 + r_p^2))$

156 The equation of the arc θ in the reference (o, x, y) is given by the relation (10) below, with the curvature
 157 radius $r_c = ED = EB$.

158 9 d) Gear Generating

159 For the generation of a complete gear wheel, the following methodology has been adopted:

160 -Codification on Matlab of the equations developed above (half of a tooth).

161 -Application of symmetry with respect to (O, ???) to get a whole tooth.

162 -Generating of N-1 others teeth by N-1 successive rotations of the initial tooth of respective angles $(2^{*}??/N)^{*}i$,
163 with $1 \leq i \leq N-1$.

164 10 e) Calculation of Radial and Axial Leakage Surfaces

165 11 i. Calculation of the border points coordinates at a given 166 position (see figures 5 and 6).

167 At a rotation angle θ around O with respect to the initial position, the coordinates of points $A1, A1',$
168 $E1, E1', B1,$ and $B1'$ (see figures 5 and 6) in $(\theta, \delta \theta, \delta \theta, \delta \theta, \delta \theta, \delta \theta)$ are given by equations
169 below: $xK = (rp * \tan(\theta)) / (\cos(\theta) + \sin(\theta) * \tan(\theta))$ $yK = xK / \tan(\theta)$ **(6)** xC
170 $= (d1 + d2) * \sin(\theta)$ $yC = (d1 + d2) * \cos(\theta)$ **(7)** $x = d$ $y = a * d$ **(8)** $xE = (rp + rc1) * \sin(\theta) +$
171 $??$ $yE = (rp + rc1) * \cos(\theta)$ **(9)** $x(q) = xE + rc1 * \sin(q)$ $y(q) = yE + rc1 * \cos(q)$ **(10)**

172 12 ?

173 $x(q) = rp * \sin(q)$ $y(q) = rp * \cos(q)$ **(11)** The coordinates of the tooth tip corner of gear in $(\theta, \delta \theta, \delta \theta, \delta \theta, \delta \theta, \delta \theta)$, $??$
174 $\delta \theta, \delta \theta, \delta \theta, \delta \theta, \delta \theta, \delta \theta$ are given by relations (14) and (15) below: $xE = rb * \tan(\theta) / (\cos(\theta) +$
175 $\sin(\theta) * \tan(\theta))$ $yE = ??? / (\cos(\theta) + \sin(\theta) * \tan(\theta))$ **(12)** $1 = ra2 * \sin(\text{inv}(\theta)) +$
176 $\text{inv}(\theta) + ??$ **(13)**

177 with $?? = \arccos(rbi/rai)$, $i=1,2$ and $\text{inv}(\theta) = \tan(\theta) - \theta$

178 With $?? = \arccos(rbi/rai)$, $i=1,2$

179 Equations (16) and (17) below are the coordinates of the pinion tooth tip corner in $(\theta, \delta \theta, \delta \theta, \delta \theta, \delta \theta, \delta \theta)$, $??$
180 $\delta \theta, \delta \theta, \delta \theta, \delta \theta, \delta \theta, \delta \theta$ $?? = ?? + \text{inv}(\theta) - \text{inv}(\theta)$, $i=1,2$ $?? = ?? + \text{inv}(\theta)$
181 $-\text{inv}(\theta)$, $i=1,2$

182 The coordinates of B_1 and B_2 in (Of, xf, yf) are given by relations (18) and (19) below:

183 When $??$, the Coordinates of the contact points between the tooth profile and the root circle are
184 given by the equation (19) below:

185 With $ay = \arccos(rb1/rp1)$;

186 Coordinates of contacts points 1 of the pinion and gear (see figure 5). Existence condition of
187 1 and 2 exists if and only if:

188 In this case, the radial surface 1 is zero: $S_{r1} = 0$ 2 exists if and only if:

189 In this case, the radial distance 2 is zero: $S_{r2} = 0$. At the initial condition, C_1 is confused with I . By applying
190 the line of contact between the two conjugate surfaces, we obtain the coordinates of points $??$ rotation angle
191 θ around O with respect to the initial position in $(\theta, \delta \theta, \delta \theta, \delta \theta, \delta \theta, \delta \theta)$, $??, \delta \theta, \delta \theta$:

192 Then the coordinates of 1 in $(\theta, \delta \theta, \delta \theta, \delta \theta, \delta \theta, \delta \theta)$ are given by the relation (22)
193 below:

194 with $?? = \tan(\theta) - \theta$; $?? = ra2 * \sin(\text{inv}(\theta)) + \text{inv}(\theta) + 2 * ?? + ??$ **(14)** $1 = ra1 * \sin(\text{inv}(\theta)) +$
195 $\text{inv}(\theta) + 2 * ?? + ??$ **(15)** $1 = ra1 * \cos(\text{inv}(\theta)) + \text{inv}(\theta) + 2 * ?? + ??$
196 $1 = ra1 * \sin(\text{inv}(\theta)) + \text{inv}(\theta) + ??$ **(16)** $1 = rb1 * \sin(\theta) + ?? + ??$ **(17)** $1 = rb1 * \cos(\theta) + ?? + ??$
197 $1 = ra1 * \sin(\text{inv}(\theta)) + \text{inv}(\theta) + ??$ **(18)** $2 = rb2 * \sin(\text{inv}(\theta)) + ?? + ??$
198 $2 = E + rb2 * \cos(\text{inv}(\theta)) + ??$
199 $2 = rp1 * \sin(\theta) + ay + ??$ **(19)** $1 = rp1 * \cos(\theta) + ay + ??$

200 $ay = \arccos(rb1/rp1)$ **(19)**
201 $\tan(\theta) - \theta = \tan(\theta) - \theta$ **(20)**
202 $\tan(\theta) - \theta = \tan(\theta) - \theta$ **(21)** $1 = rb1 * (\theta + \text{inv}(\theta)) \sin(\text{Arctan}(\theta)) + \text{inv}(\theta)$
203 $1 = rb1 * (\theta + \text{inv}(\theta)) \cos(\text{Arctan}(\theta)) + \text{inv}(\theta)$ **(22)**

204 The coordinates of 2 in $(\theta, \delta \theta, \delta \theta, \delta \theta, \delta \theta, \delta \theta)$ are given by the relation (23) below:

205 with $?? = \tan(\theta) - \theta$;

206 In $(\theta, \delta \theta, \delta \theta, \delta \theta, \delta \theta, \delta \theta)$, the coordinates of 1 are given by the relation (24) below:

207 with $?? = \tan(\theta) - \theta$;

208 In (Op, xp, yp) , the coordinates of 2 are given by the relation (25) below:

209 with $?? = \tan(\theta) + 2 * ?? + ??$; $?? = rb1 * (\theta + \text{inv}(\theta))$; $?? = rb2 * (\theta + \text{inv}(\theta))$
210 $?? = rb1 * (\theta + \text{inv}(\theta))$; $?? = rb2 * (\theta + \text{inv}(\theta))$

211 ii.

13 Calculation of Radial Leakage Surfaces

The radial leakage surfaces vary in function of the rotation angle of gear. For the calculation of radial leakage surfaces we will distinguish 05 possibilities:

-When α_1 and α_2 exists, i.e., when the profiles touch each other simultaneously. In this case the surfaces S_{r1} and S_{r2} are simultaneously zero. -When we are at the left of the initial position, and only α_2 exists ($S_{r1} > 0$ and $S_{r2} = 0$), -When we are at the left of the initial position with α_1 and α_2 does not exist ($S_{r1} > 0$ and $S_{r2} > 0$), -When we are at the right of the initial position and only α_2 exists ($S_{r1} = 0$ and $S_{r2} > 0$), -When we are at the right of the initial position with α_1 and α_2 does not exist ($S_{r1} > 0$ and $S_{r2} > 0$), The relations below give the expressions of the radial leakage surfaces in each of these cases cited above.

14 At the right of the initial position

Case where $S_{r1} = 0$ and $S_{r2} > 0$: $(\tan(\alpha_0) - (\alpha_1 \alpha_2)) / (\alpha_1 \alpha_2) > \alpha_1 < \alpha_2$ ($\alpha_1 < \alpha_2$) ($\tan(\alpha_0) - (\alpha_1 \alpha_2) > \alpha_1 < \alpha_2$)

According to figure 5, where b is the face of the tooth width.
with $\alpha_2 \alpha_1 = \alpha_1 \alpha_2$, $\alpha_1 \alpha_2 = \alpha_1 \alpha_2$, with $\text{mes}(\alpha_1, \alpha_2) = \arccos(((x_2 - 0)(1-0)) / \alpha_1 \alpha_2)$ and $\text{mes}(\alpha_1, \alpha_2) = \arccos(((x_1 - 0)(1-0)) / \alpha_1 \alpha_2)$. $\alpha_1 \alpha_2 = rb_1 * (\alpha_1 + \alpha_2) \sin(\arctan(\alpha_2)) + \alpha_2 \alpha_1 \alpha_2$ (23) $\alpha_1 \alpha_2 = rb_1 * (\alpha_1 + \alpha_2) \sin(\arctan(\alpha_2)) + \alpha_2 \alpha_1 \alpha_2$ (23) $\alpha_1 \alpha_2 = rb_2 * (\alpha_1 + \alpha_2) \sin(\arctan(\alpha_2)) + \alpha_2 \alpha_1 \alpha_2$ (24) $\alpha_1 \alpha_2 = rb_2 * (\alpha_1 + \alpha_2) \sin(\arctan(\alpha_2)) + \alpha_2 \alpha_1 \alpha_2$ (25) $S_{r2} = \alpha_1 \alpha_2$ (26) $\alpha_1 \alpha_2 = \alpha_1 \alpha_2$ (27) $\alpha_1 \alpha_2 = \text{mes}(\alpha_1, \alpha_2) - \text{mes}(\alpha_1, \alpha_2)$ and $\text{mes}(\alpha_1, \alpha_2) = \text{mes}(\alpha_1, \alpha_2)$ (28)

Establishment of an Analytical Model for Determining Leakage Surfaces in an External Tooth Spur Gear

15 Global Journal of Researches in Engineering

(A) Volume Xx XII Issue II V ersion I

Case where $S_{r1} > 0$ and $S_{r2} > 0$: $(\alpha_1 < \tan(\alpha_0) - (\alpha_1 \alpha_2)) / (\alpha_1 \alpha_2) > \alpha_1 < \alpha_2$
According to figure 6, $\alpha_1 \alpha_2 = \alpha_1 \alpha_2$, $\alpha_1 \alpha_2 = \alpha_1 \alpha_2$, $\alpha_1 \alpha_2 = \text{mes}(\alpha_1, \alpha_2)$ with $\text{mes}(\alpha_1, \alpha_2) = \arccos(((x_2 - 0)(1-0)) / \alpha_1 \alpha_2)$ and $\text{mes}(\alpha_1, \alpha_2) = \arccos(((x_1 - 0)(1-0)) / \alpha_1 \alpha_2)$
 S_{r1} is given by the relation ($\alpha_1 \alpha_2$)

16 At the left of the initial position

Case where $S_{r1} > 0$ and $S_{r2} = 0$: $(\tan(\alpha_0) + \alpha_1 \alpha_2) / (\alpha_1 \alpha_2) > \alpha_1 > \alpha_2$ ($\tan(\alpha_0) - (\alpha_1 \alpha_2) > \alpha_1 > \alpha_2$)

Like the previous cases, with $\alpha_1 \alpha_2 = \alpha_1 \alpha_2$, $\alpha_1 \alpha_2 = \alpha_1 \alpha_2$, $\alpha_1 \alpha_2 = \text{mes}(\alpha_1, \alpha_2)$ and $\text{mes}(\alpha_1, \alpha_2) = \arccos(((x_2 - 0)(1-0)) / \alpha_1 \alpha_2)$ and $\text{mes}(\alpha_1, \alpha_2) = \arccos(((x_1 - 0)(1-0)) / \alpha_1 \alpha_2)$
Case where $S_{r1} > 0$ and $S_{r2} > 0$: $(\alpha_1 > \tan(\alpha_0) + \alpha_1 \alpha_2) / (\alpha_1 \alpha_2) > \alpha_1 > \alpha_2$ with $\alpha_1 \alpha_2 = \alpha_1 \alpha_2$, $\alpha_1 \alpha_2 = \alpha_1 \alpha_2$, $\alpha_1 \alpha_2 = \text{mes}(\alpha_1, \alpha_2)$ and $\text{mes}(\alpha_1, \alpha_2) = \arccos(((x_2 - 0)(1-0)) / \alpha_1 \alpha_2)$ and $\text{mes}(\alpha_1, \alpha_2) = \arccos(((x_1 - 0)(1-0)) / \alpha_1 \alpha_2)$
 S_{r1} is given by relation (33)

iii. Calculation of Axial Leakage Surfaces Case where $S_{r1} = 0$ and $S_{r2} = 0$: $(\alpha_1 \alpha_2) / (\alpha_1 \alpha_2) > \alpha_1 > \alpha_2$ ($\tan(\alpha_0) - (\alpha_1 \alpha_2) > \alpha_1 > \alpha_2$)

Case where $\alpha_1 < \alpha_2$ According to figure 5 and figure 6: $S_{r1} = \alpha_1 \alpha_2$ (29) $\alpha_1 \alpha_2 = \alpha_1 \alpha_2$ (30) $\text{mes}(\alpha_1, \alpha_2) = \text{mes}(\alpha_1, \alpha_2)$ (31) $S_{r1} = \alpha_1 \alpha_2$ (32) $\alpha_1 \alpha_2 = \alpha_1 \alpha_2$ (33) $S_{r2} = \alpha_1 \alpha_2$ (35)

(36) Surface axiale = $S_{r1} \alpha_1 \alpha_2 = S_{r1} \alpha_1 \alpha_2$ (37) $\text{mes}(\alpha_1, \alpha_2) = \text{mes}(\alpha_1, \alpha_2)$ (38) $\text{mes}(\alpha_1, \alpha_2) = \text{mes}(\alpha_1, \alpha_2)$ (39) $\text{mes}(\alpha_1, \alpha_2) = \text{mes}(\alpha_1, \alpha_2)$ (40) $\text{mes}(\alpha_1, \alpha_2) = \text{mes}(\alpha_1, \alpha_2)$ (41) $\text{mes}(\alpha_1, \alpha_2) = \text{mes}(\alpha_1, \alpha_2)$ (42) $\text{mes}(\alpha_1, \alpha_2) = \text{mes}(\alpha_1, \alpha_2)$ (43) $\text{mes}(\alpha_1, \alpha_2) = \text{mes}(\alpha_1, \alpha_2)$ (44) $\text{mes}(\alpha_1, \alpha_2) = \text{mes}(\alpha_1, \alpha_2)$ (45) $\text{mes}(\alpha_1, \alpha_2) = \text{mes}(\alpha_1, \alpha_2)$ (46) $\text{mes}(\alpha_1, \alpha_2) = \text{mes}(\alpha_1, \alpha_2)$ (47) $\text{mes}(\alpha_1, \alpha_2) = \text{mes}(\alpha_1, \alpha_2)$ (48) $\text{mes}(\alpha_1, \alpha_2) = \text{mes}(\alpha_1, \alpha_2)$ (49) $\text{mes}(\alpha_1, \alpha_2) = \text{mes}(\alpha_1, \alpha_2)$ (50) $\text{mes}(\alpha_1, \alpha_2) = \text{mes}(\alpha_1, \alpha_2)$ (51) $\text{mes}(\alpha_1, \alpha_2) = \text{mes}(\alpha_1, \alpha_2)$ (52) $\text{mes}(\alpha_1, \alpha_2) = \text{mes}(\alpha_1, \alpha_2)$ (53) $\text{mes}(\alpha_1, \alpha_2) = \text{mes}(\alpha_1, \alpha_2)$ (54) $\text{mes}(\alpha_1, \alpha_2) = \text{mes}(\alpha_1, \alpha_2)$ (55) $\text{mes}(\alpha_1, \alpha_2) = \text{mes}(\alpha_1, \alpha_2)$ (56) $\text{mes}(\alpha_1, \alpha_2) = \text{mes}(\alpha_1, \alpha_2)$ (57) $\text{mes}(\alpha_1, \alpha_2) = \text{mes}(\alpha_1, \alpha_2)$ (58) $\text{mes}(\alpha_1, \alpha_2) = \text{mes}(\alpha_1, \alpha_2)$ (59) $\text{mes}(\alpha_1, \alpha_2) = \text{mes}(\alpha_1, \alpha_2)$ (60) $\text{mes}(\alpha_1, \alpha_2) = \text{mes}(\alpha_1, \alpha_2)$ (61) $\text{mes}(\alpha_1, \alpha_2) = \text{mes}(\alpha_1, \alpha_2)$ (62) $\text{mes}(\alpha_1, \alpha_2) = \text{mes}(\alpha_1, \alpha_2)$ (63) $\text{mes}(\alpha_1, \alpha_2) = \text{mes}(\alpha_1, \alpha_2)$ (64) $\text{mes}(\alpha_1, \alpha_2) = \text{mes}(\alpha_1, \alpha_2)$ (65) $\text{mes}(\alpha_1, \alpha_2) = \text{mes}(\alpha_1, \alpha_2)$ (66) $\text{mes}(\alpha_1, \alpha_2) = \text{mes}(\alpha_1, \alpha_2)$ (67) $\text{mes}(\alpha_1, \alpha_2) = \text{mes}(\alpha_1, \alpha_2)$ (68) $\text{mes}(\alpha_1, \alpha_2) = \text{mes}(\alpha_1, \alpha_2)$ (69) $\text{mes}(\alpha_1, \alpha_2) = \text{mes}(\alpha_1, \alpha_2)$ (70) $\text{mes}(\alpha_1, \alpha_2) = \text{mes}(\alpha_1, \alpha_2)$ (71) $\text{mes}(\alpha_1, \alpha_2) = \text{mes}(\alpha_1, \alpha_2)$ (72) $\text{mes}(\alpha_1, \alpha_2) = \text{mes}(\alpha_1, \alpha_2)$ (73) $\text{mes}(\alpha_1, \alpha_2) = \text{mes}(\alpha_1, \alpha_2)$ (74) $\text{mes}(\alpha_1, \alpha_2) = \text{mes}(\alpha_1, \alpha_2)$ (75) $\text{mes}(\alpha_1, \alpha_2) = \text{mes}(\alpha_1, \alpha_2)$ (76) $\text{mes}(\alpha_1, \alpha_2) = \text{mes}(\alpha_1, \alpha_2)$ (77) $\text{mes}(\alpha_1, \alpha_2) = \text{mes}(\alpha_1, \alpha_2)$ (78) $\text{mes}(\alpha_1, \alpha_2) = \text{mes}(\alpha_1, \alpha_2)$ (79) $\text{mes}(\alpha_1, \alpha_2) = \text{mes}(\alpha_1, \alpha_2)$ (80) $\text{mes}(\alpha_1, \alpha_2) = \text{mes}(\alpha_1, \alpha_2)$ (81) $\text{mes}(\alpha_1, \alpha_2) = \text{mes}(\alpha_1, \alpha_2)$ (82) $\text{mes}(\alpha_1, \alpha_2) = \text{mes}(\alpha_1, \alpha_2)$ (83) $\text{mes}(\alpha_1, \alpha_2) = \text{mes}(\alpha_1, \alpha_2)$ (84) $\text{mes}(\alpha_1, \alpha_2) = \text{mes}(\alpha_1, \alpha_2)$ (85) $\text{mes}(\alpha_1, \alpha_2) = \text{mes}(\alpha_1, \alpha_2)$ (86) $\text{mes}(\alpha_1, \alpha_2) = \text{mes}(\alpha_1, \alpha_2)$ (87) $\text{mes}(\alpha_1, \alpha_2) = \text{mes}(\alpha_1, \alpha_2)$ (88) $\text{mes}(\alpha_1, \alpha_2) = \text{mes}(\alpha_1, \alpha_2)$ (89) $\text{mes}(\alpha_1, \alpha_2) = \text{mes}(\alpha_1, \alpha_2)$ (90) $\text{mes}(\alpha_1, \alpha_2) = \text{mes}(\alpha_1, \alpha_2)$ (91) $\text{mes}(\alpha_1, \alpha_2) = \text{mes}(\alpha_1, \alpha_2)$ (92) $\text{mes}(\alpha_1, \alpha_2) = \text{mes}(\alpha_1, \alpha_2)$ (93) $\text{mes}(\alpha_1, \alpha_2) = \text{mes}(\alpha_1, \alpha_2)$ (94) $\text{mes}(\alpha_1, \alpha_2) = \text{mes}(\alpha_1, \alpha_2)$ (95) $\text{mes}(\alpha_1, \alpha_2) = \text{mes}(\alpha_1, \alpha_2)$ (96) $\text{mes}(\alpha_1, \alpha_2) = \text{mes}(\alpha_1, \alpha_2)$ (97) $\text{mes}(\alpha_1, \alpha_2) = \text{mes}(\alpha_1, \alpha_2)$ (98) $\text{mes}(\alpha_1, \alpha_2) = \text{mes}(\alpha_1, \alpha_2)$ (99) $\text{mes}(\alpha_1, \alpha_2) = \text{mes}(\alpha_1, \alpha_2)$ (100)

273 $?? 1 ?? 2 = 0.5 * ?? 2 * (2 * ?? 2), S?? 2 ?? 1 ?? 1 ?? 2 = 0.5 * ?? 2 ((? (?? ?? 2 ?? ?? 2) 2 ? 1) 3$
 274 $- ?? ?? 2 3) / 3$ and $S?? 2 ?? 2 ??? 1 ?? 2 = 0.5 * ?? 2 * ((? (?? ?? 2 ?? ?? 2) 2 ? 1) 3 - ??? ?? 2 3) / 3$ with $S??$
 275 $1 ?? 1 ?? 1 ?? 1 = 0.5 * r_{b1} 2 * (?? ?? 1 3) / 3$, $SO 1 B 1 B ? 1 O 1 = (rc1 + rp1) * o1c * \sin(?) - rc1 2 * (q_{max} - q_{min}) +$
 276 $rp1 2 * (q_{2max} - q_{2min}) ?? 1 c = (?? ?? ? 0) 2 + (?? ??) 2 q_{2max} = (? / 2) - (? + ? s)$ and $q_{2min} = (? / 2) - (? / N1)$
 277 $q_{min} = \text{Arccos}((1 * (?? ?? - ?? ??) + 0 * (?? ?? - ?? ??)) / EB)$ and $q_{max} = q_{min} + \text{acos}(((?? ?? - ?? ??) * (?? ?? - ??$
 278 $??) + (?? ?? - ?? ??) * (?? ?? - ?? ??)) / rc1 2)$ $SO 1 B ? 1 C 2 O 1 = 0.5 * r_{b1} 2 * (? C 2 3) / 3$.

279 ? Case where ?? ?? ? ?? ?? According to figures 5 and 6 Figure 8 below is a detailed view of the half of the
 280 tooth profile taken from the simulation result for the specific case of gear 1 in table 1. $S?? 1 ?? 1 ?? 1 ??? 1 ??$
 281 $2 ?? 1 = \text{triangle}_?? 1 ?? 2 ?? 2 ?? 1 - \text{triangle}_?? 1 ?? 1 ?? 2 ?? 1 - S?? 2 ?? 2 ?? 1 ??? 1 ?? 1 ?? 2 (38)$ $S?? 2$
 282 $?? 2 ?? 1 ??? 1 ?? 1 ?? 2 = S?? 2 ?? 2 ??? 1 ?? 2 + S?? 2 ?? 2 ??? 1 ?? 1 ?? 2 + S?? 2 ?? 1 ?? 1 ?? 2 (39)$
 283 $S?? 1 ?? 1 ?? 1 ??? 1 ?? 2 ?? 1 = S?? 1 ?? 1 ?? 1 ?? 1 + S?? 1 ?? 1 ??? 1 ?? 1 + S?? 1 ??? 1 ?? 1 ?? 2 ?? 1 (40)$
 284 Surface axiale = $S?? 1 ?? 1 ?? 1 ??? 2 ?? 1 ??? 1 ?? 1 = S?? 1 ?? 1 ?? 1 ??? 1 ?? 2 ?? 1 - S?? 1 ?? 1 ?? 1 ?? 1 ??$
 285 $1 ??? 2 ?? 1 (41)$ $S?? 1 ?? 1 ?? 1 ?? 1 ??? 2 ?? 1 = S?? 1 ?? 1 ??? 2 ?? 1 + S?? 1 ?? 1 ?? 1 ??? 1 + S?? 1 ??$
 286 $1 ?? 1 ?? 1 (42)$ with $S?? 1 ?? 1 ??? 2 ?? 1 = 0.5 * r_{b1} 2 * ((? C 2 3) - ? rp 1 3) / 3, S?? 1 ?? 1 ?? 1 ??? 1 = rp1 2$
 287 $* (q_{3max} - q_{2min})$ and $q_{3max} = \text{Arctan}(yp1 / xp1)$ $S?? 1 ?? 1 ?? 1 ?? 1 = 0.5 * rp1 2 * (?? 1 3 - ? rp 1 3) / 3$ with ?
 288 $rp 1 = ? (?? ?? 1 ?? ?? 1) 2 ? 1$

289 The particularity here is the presence of a straight part on our teeth, namely the segment [BC]. Figure ??
 290 below is a detailed view of the half of the tooth profile taken from the simulation result for the specific case of
 291 gear 2 in table 1.

292 The profile is made up of the tooth top, the involute part, the circular part, and tooth root. Here, the straight
 293 part no longer exists.

294 A detailed view of the half of the tooth profile resulting from the simulation result for the particular case of
 295 gear 3 of table 1 is represented in figure 10 below. Case of the gearing system of table 2 The result of our model
 296 for calculating the pockets volumes corresponding to the gearing system of table 2 has generated the curve of
 297 figure 12

298 17 b) Results of Calculations of Radial and Axial Leakage 299 Surfaces

300 To validate our model, the simulation of our equations and formulas developed above (equations (13) to (42)) on
 301 Matlab 16 was carried out with the particular case of a gear whose characteristics are grouped in table 2 below.
 302 The application of our model for calculating of the radial leakage surfaces 1 and 2 relative to the gear of table 2
 303 has generated the curves of figure 11

304 18 c) Results Interpretation

305 The curves of Figure 11 justify the similarity of the radial and axial leakage surfaces on each side of the initial
 306 position ($?? 1 = 0$). This result agrees with the surfaces evolution of figure 2. we observe that On figures 2.a)
 307 to 2.h) the axial surface reaches its minimum at the initial position ($?? 1 = 0$). This observation agrees with the
 308 curve of figure 12.

309 More we move away from the initial position ($?? 1 = 0$), the pockets volumes increase. This result agrees with
 310 the observation of figures 2.a) to 2.h).

311 The curves in figure 11 show that at the left of the initial position, the radial leakage surface one is always
 312 greater than the radial leakage surface two and, at the right of the initial position, it is the opposite phenomenon.
 313 This result agrees with the observations of figure 2.

314 In figure 11, the two profiles bordering the radial surface 1 ($?? ?? 1$) meet when $?? 1$ belongs in the interval
 315 $[-3,75^\circ; 6,5^\circ]$. For the radial surface 2 ($?? ?? 2$), this phenomenon occurs in the interval $[-6,5^\circ; 3,75^\circ]$.

316 19 V. Model Validation

317 The validation of our model follows from a comparative study between the results of our model and the results of
 318 Abdelilah Lasri and al [13] and Diab Y. and al [10] for the same gear system. We have superimposed the curves
 319 of our model and those of the reference models. a) Superposition of the Radial Surfaces Curves of our Model and
 320 those Resulting from the Model of Abdelilah Lasri [13] Figure 13 below is the result of the superposition of the
 321 radial leakage surfaces (Sr1 and Sr2). In this figure, the leakage surfaces curves of our model are in blue colour
 322 and the curves of Abdelilah Lasri's model [13] are in red.

323 Rotation angle of driver gear in degree pocketVolume in m b) Superposition of Pocket Volume Curves from
 324 our Model and those from the Diab's Model [10] Figure 14 below is the result of the superposition of pocket
 325 volumes. On this figure, the curve of pocket volumes from our model is blue and the Diab's model curve [10] is
 326 black. The curves of the figures 13 and 14 and the relative deviations between the results from our model and
 327 the reference models allow us to state with certainty that the model developed in this work is valid and meets
 328 our set objectives. The model developed in this work allows us to calculate the exact values of the axial and
 329 radial leakage surfaces of the lubricant in a gear.

20 VI. Conclusion

330

331 A better optimization of the power losses by the lubricant trapping in the inter-tooth space requires a preliminary
332 work of total lifting of the veil on the gear inter-tooth space during the movement. In this perspective, we have
333 established a purely analytical model allowing to accurately evaluating the radial and axial leakage surfaces of
334 the lubricant in the inter-tooth space of external spur gears.

335

336 This model was developed based on the parametric equations of a tooth profile and the exploitation of
337 the involute properties, followed by the surface integrations delimited by the contour representing their exact
338 boundary. The results are presented as curves of the evolution of the leakage surfaces (radial and axial) as a
339 function of the driving gear's rotation angle. The curve of the evolution of the axial leakage surfaces as a function
340 of the rotation angle is a symmetrical parabola, and the two curves of the evolution of the radial leakage surfaces
341 are symmetrical (relative to each other). These results agree with the observation of the lubricant behavior in
342 the inter-tooth space during gear movement. Far from numerical approximations, this model is an analytical
343 formula allowing us to evaluate the exact leakage surfaces directly, according to the geometrical parameters of
the gears.

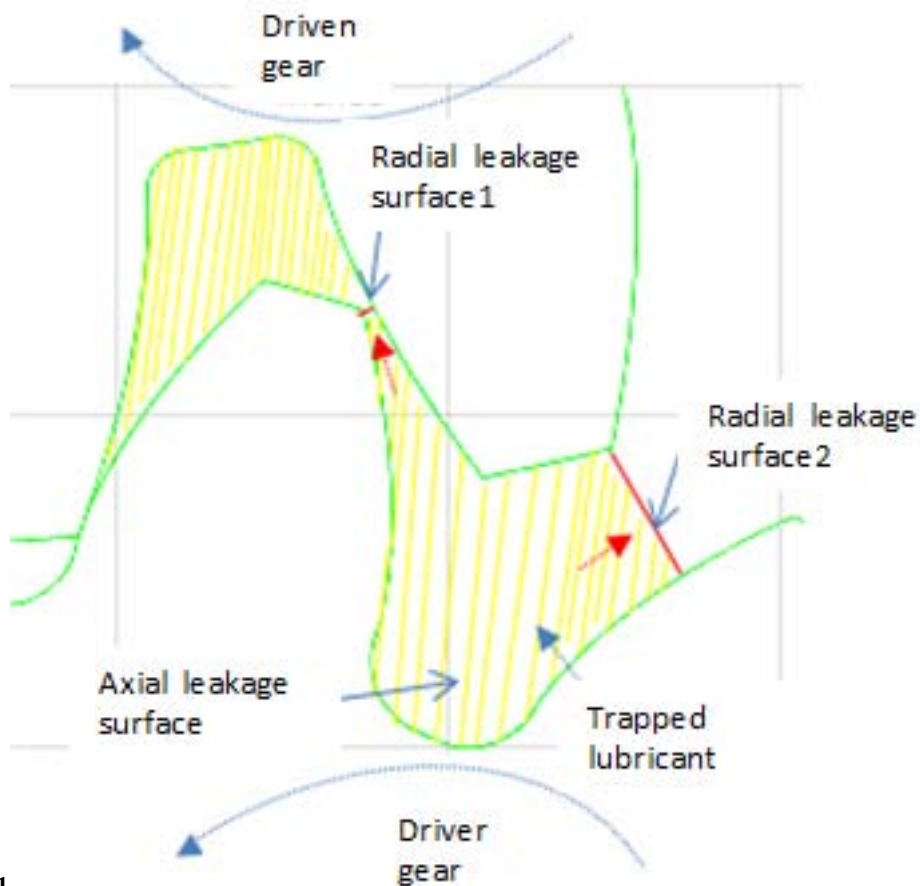


Figure 1: Figure 1 :

343

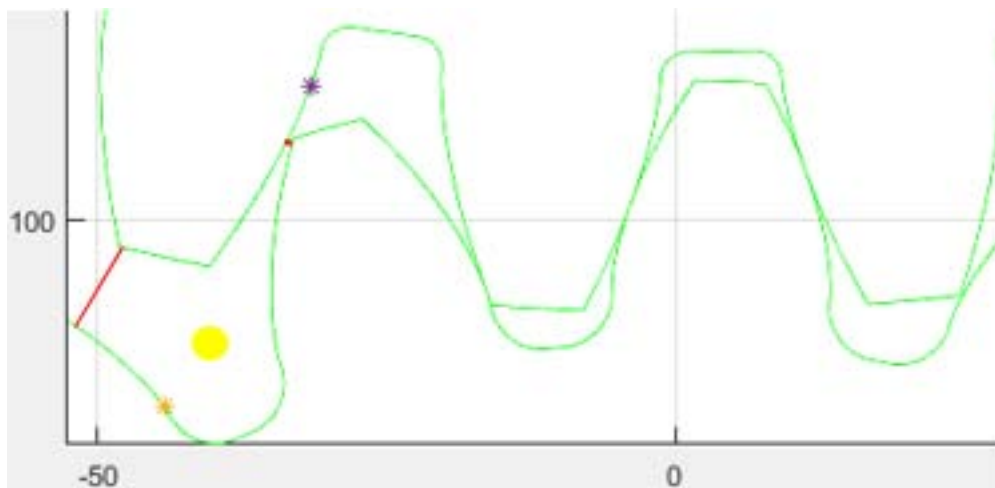


Figure 2: pinion

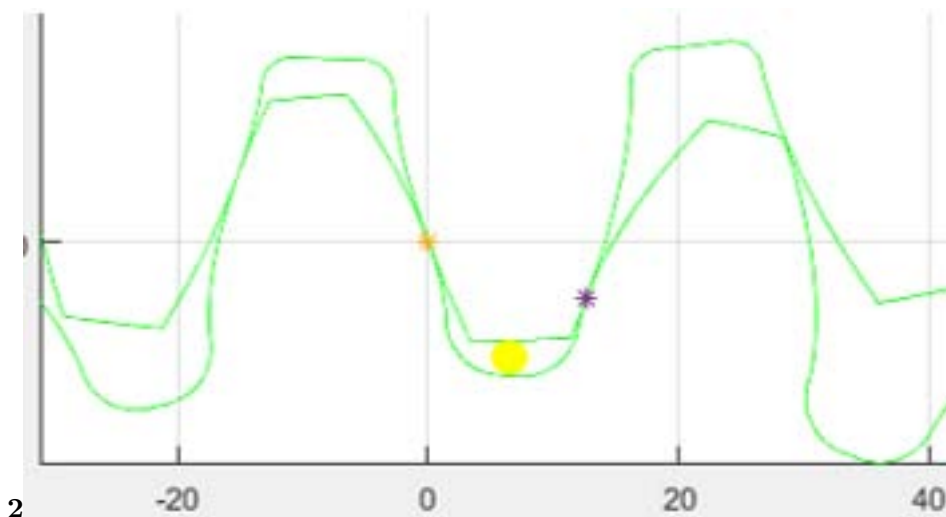


Figure 3: Figure 2 :

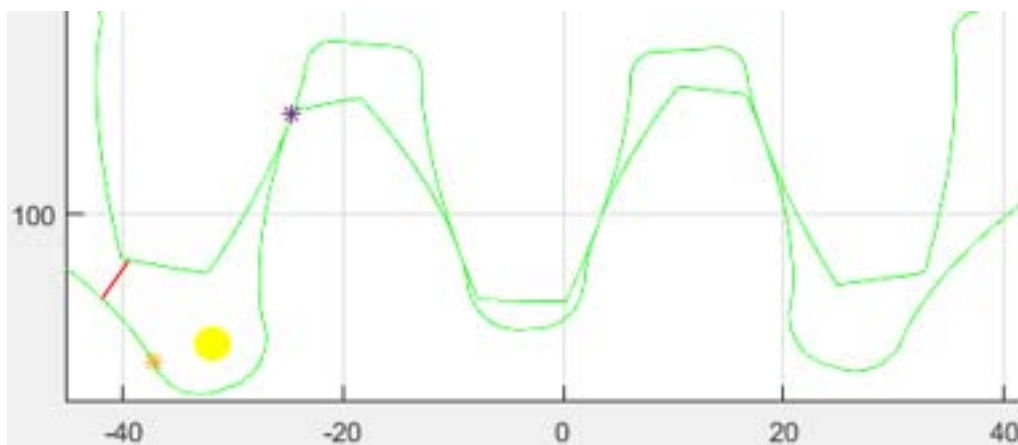


Figure 4:

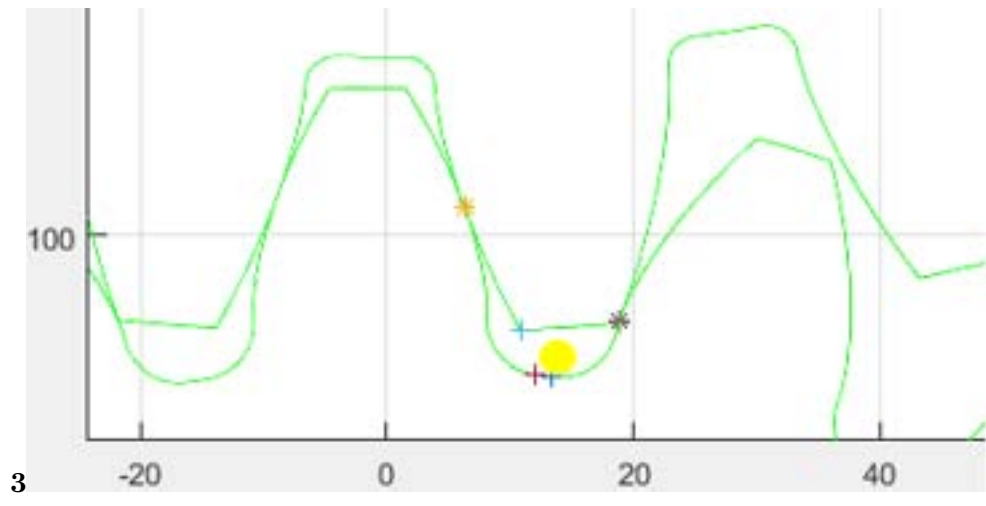


Figure 5: Figure 3 :

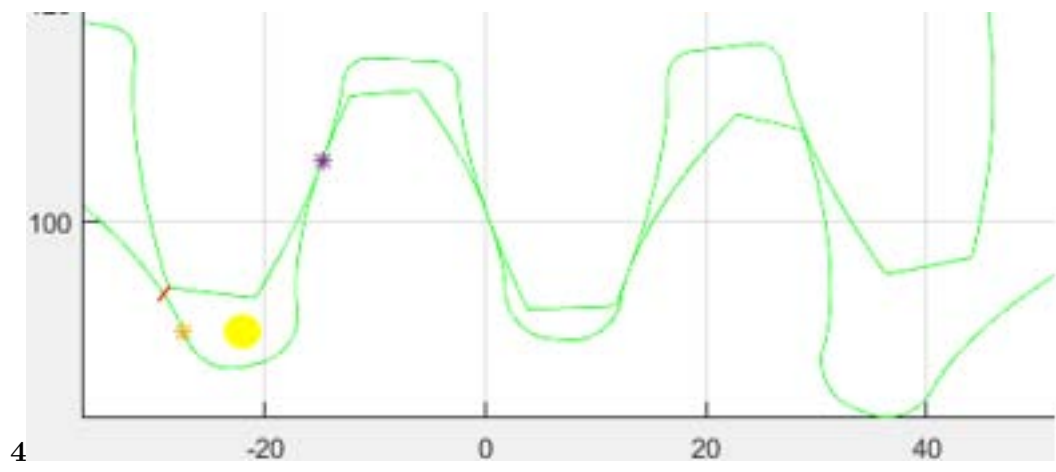


Figure 6: Figure 4

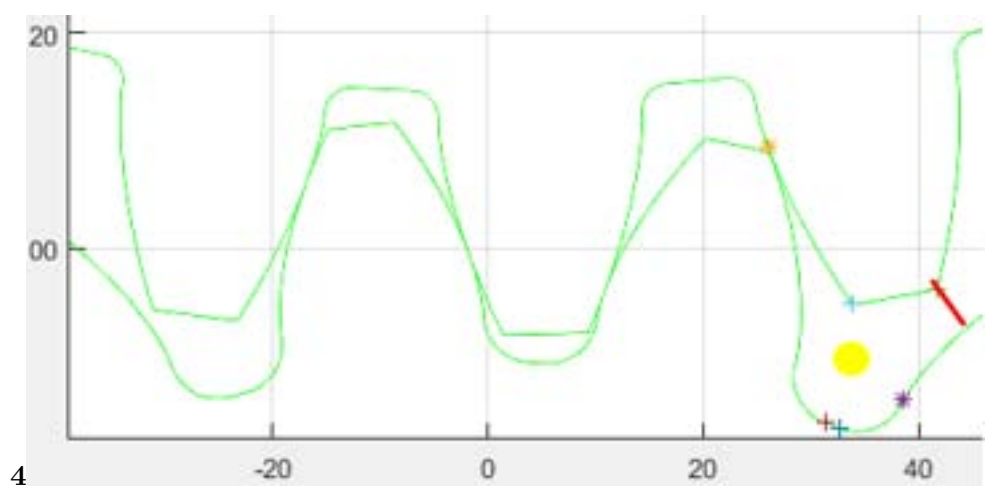


Figure 7: Figure 4 :

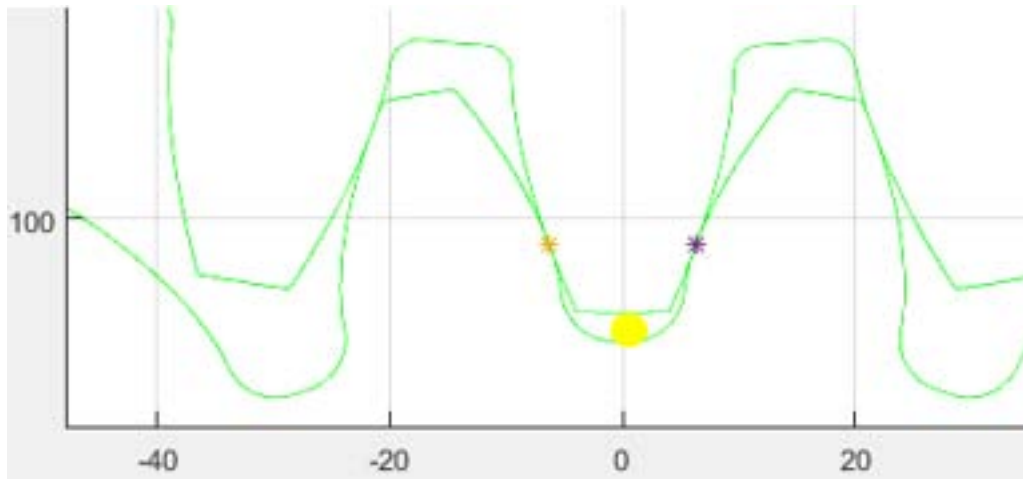


Figure 8:

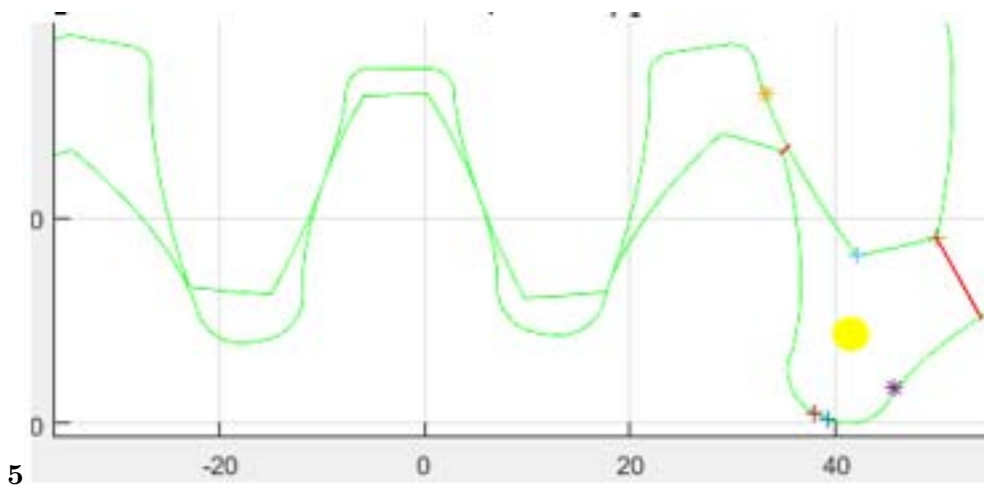
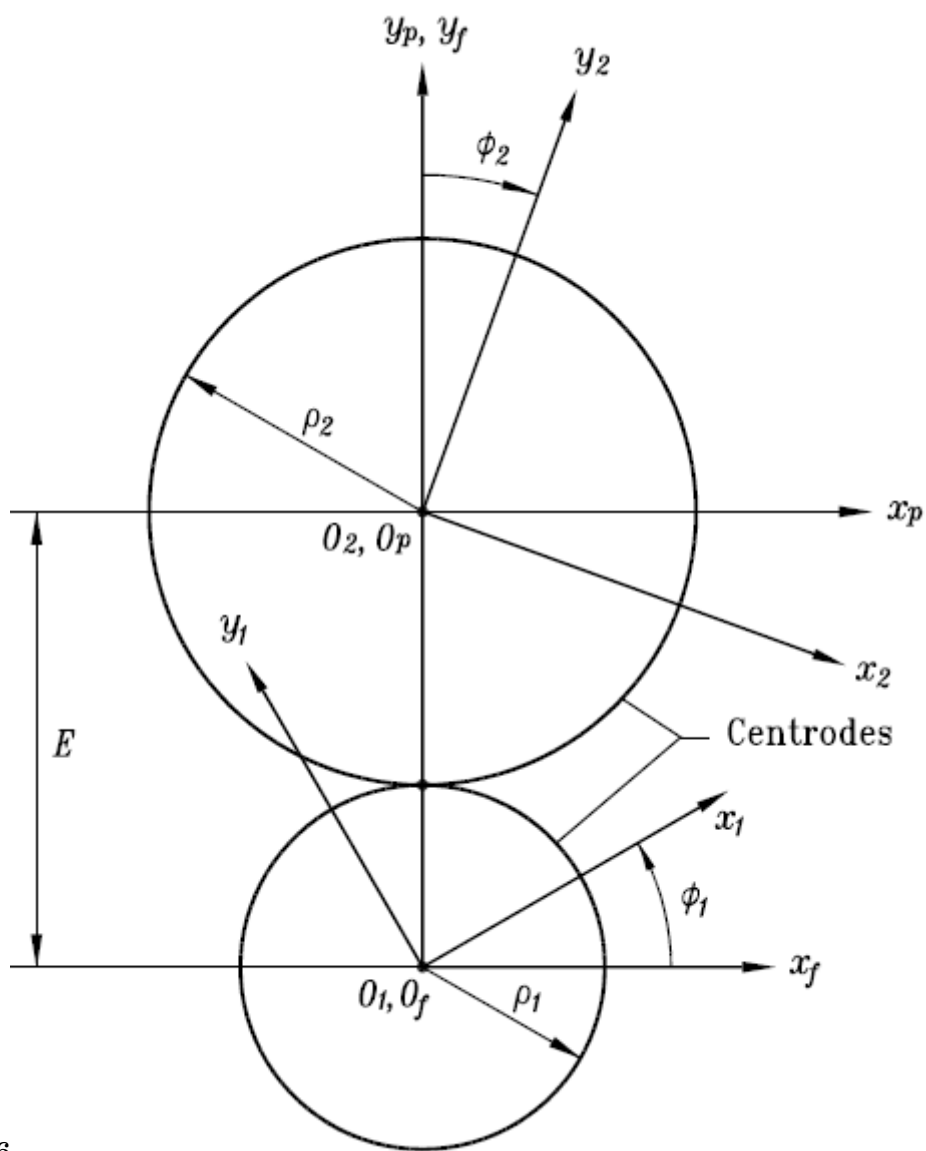


Figure 9: Figure 5 :



6

Figure 10: Figure 6 :

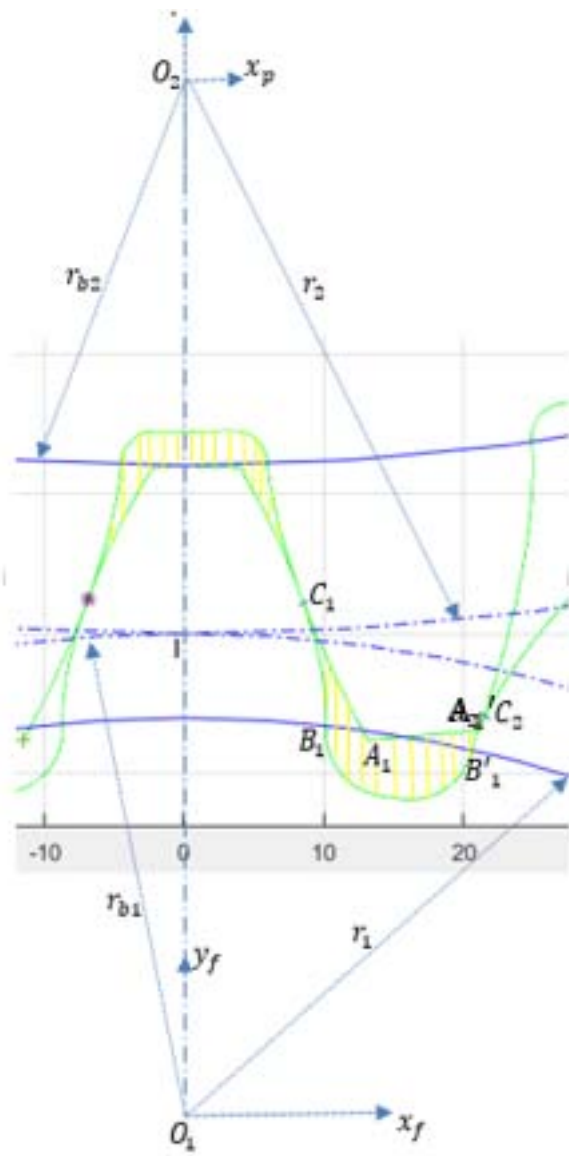


Figure 12:

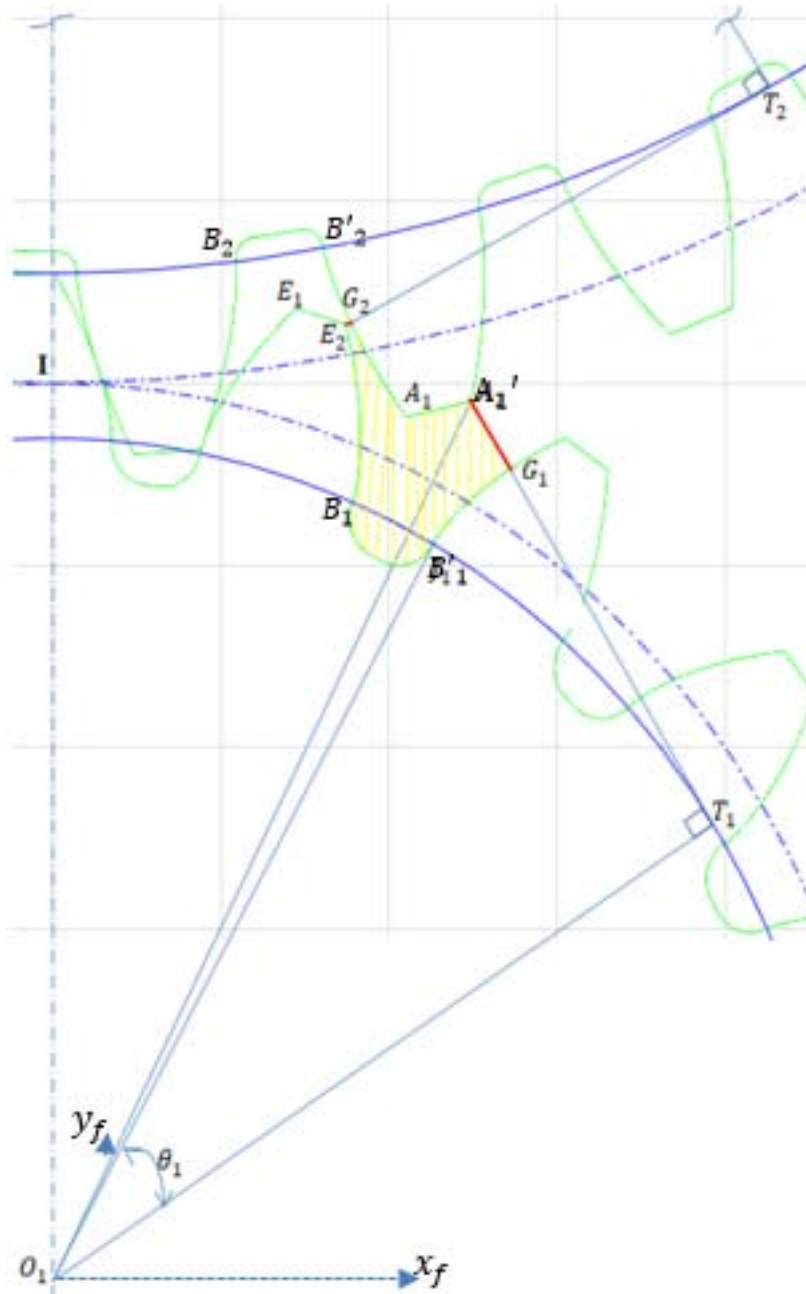
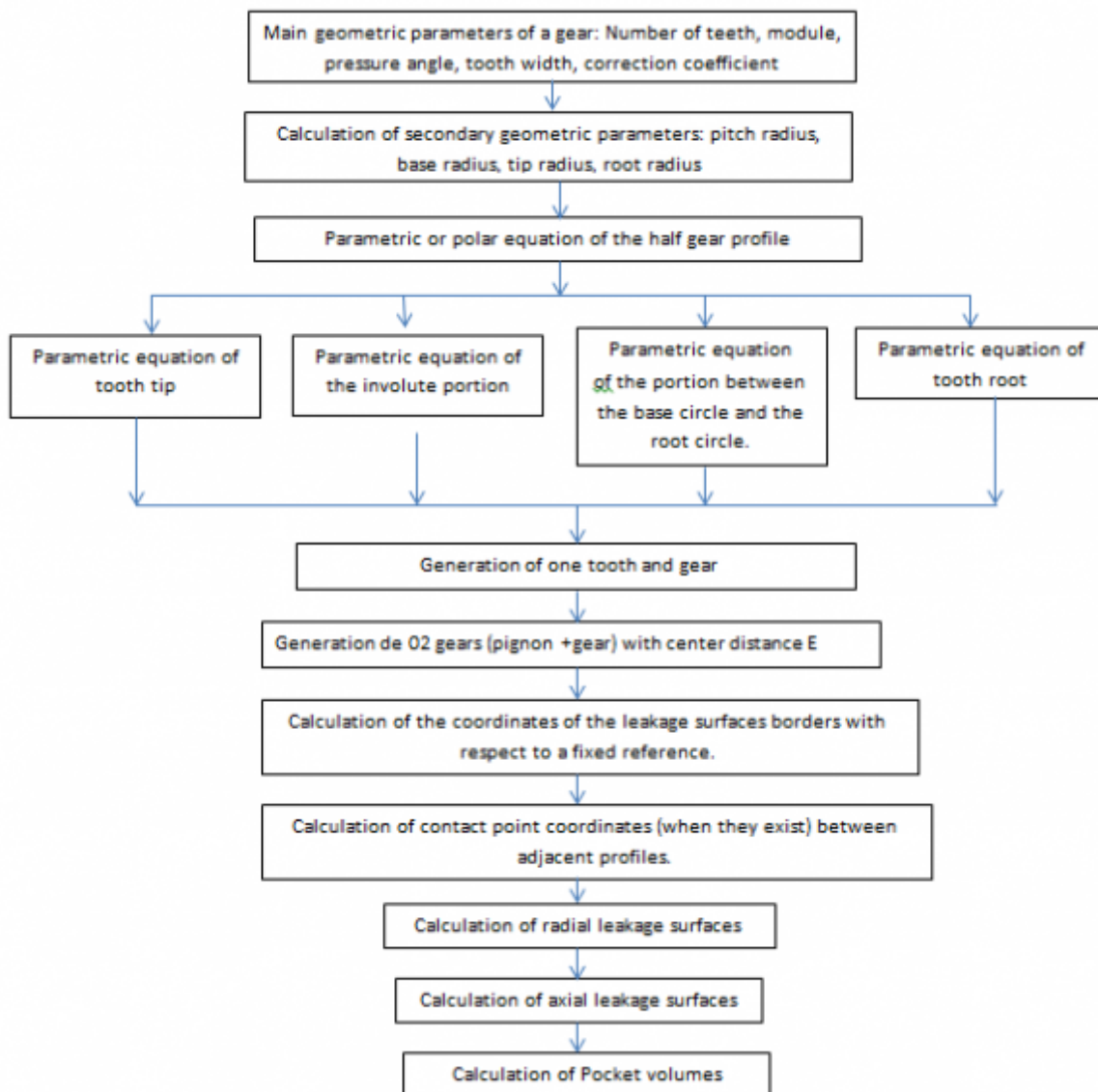
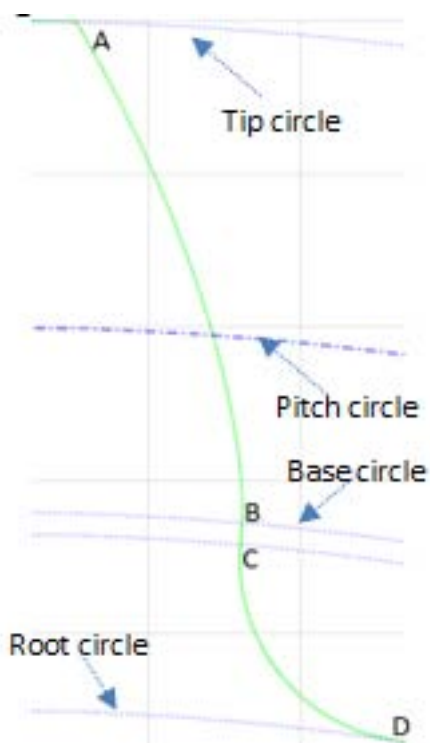


Figure 13:



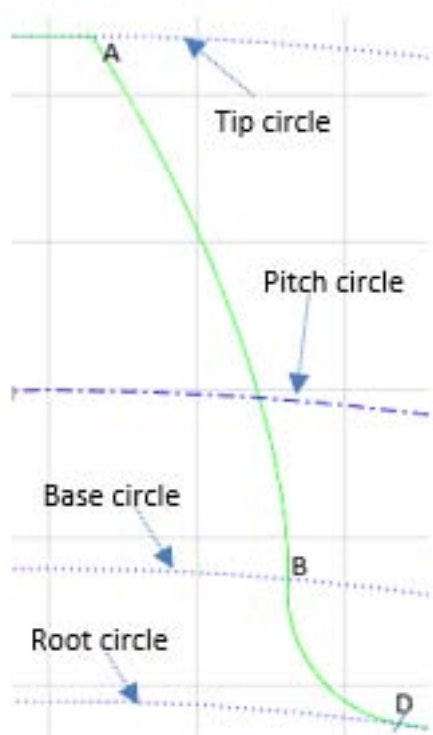
8

Figure 14: Figure 8 :



910

Figure 15: Figure 9 :Figure 10 :



11

Figure 16: Figure 11 :

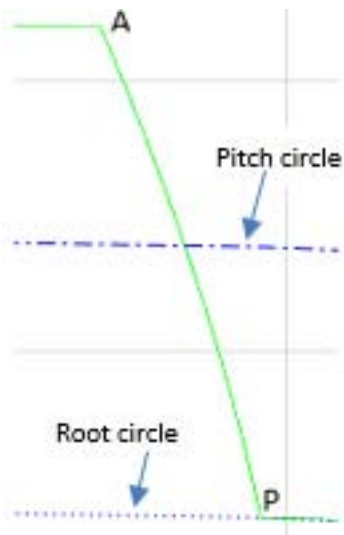


Figure 17:

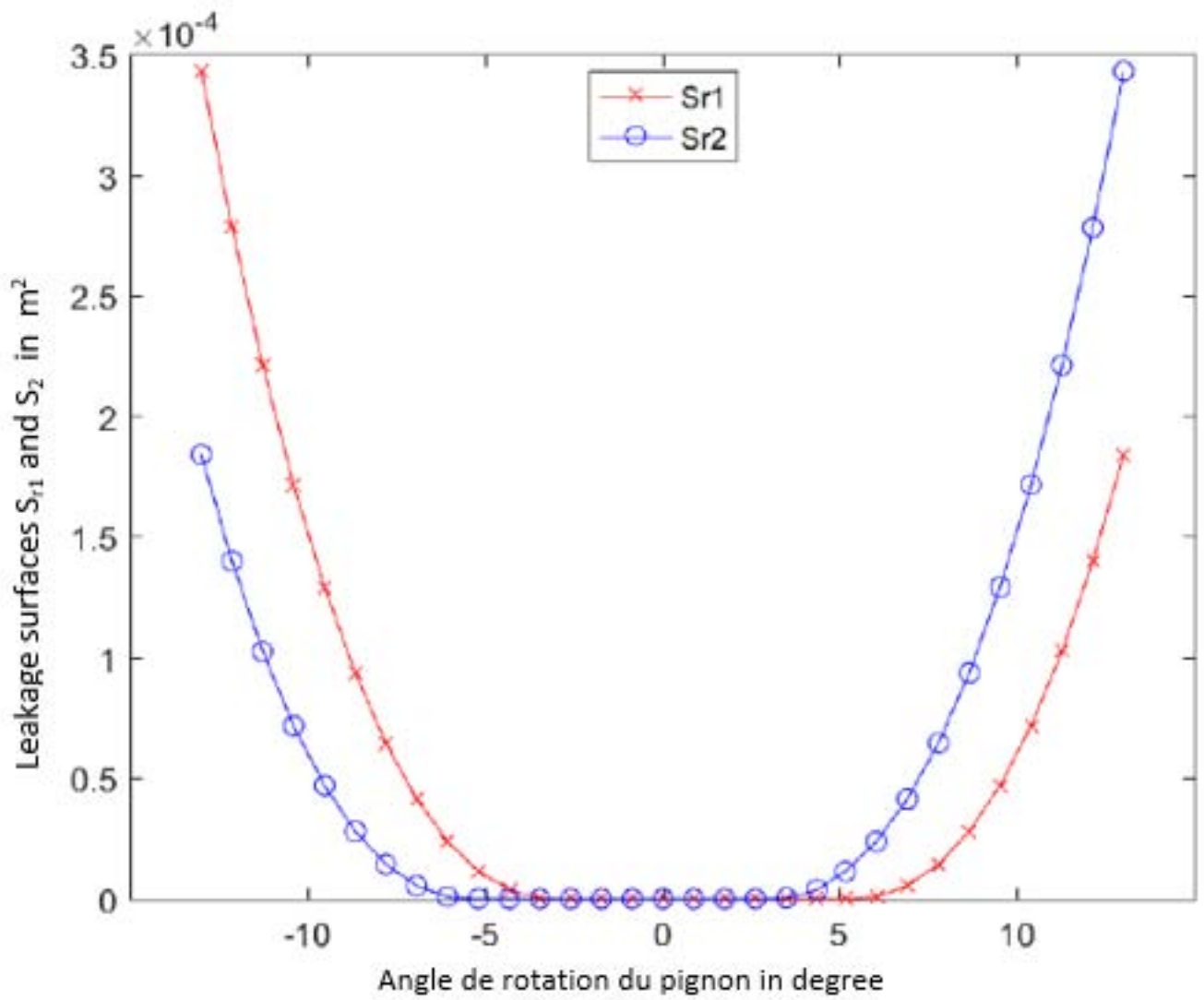
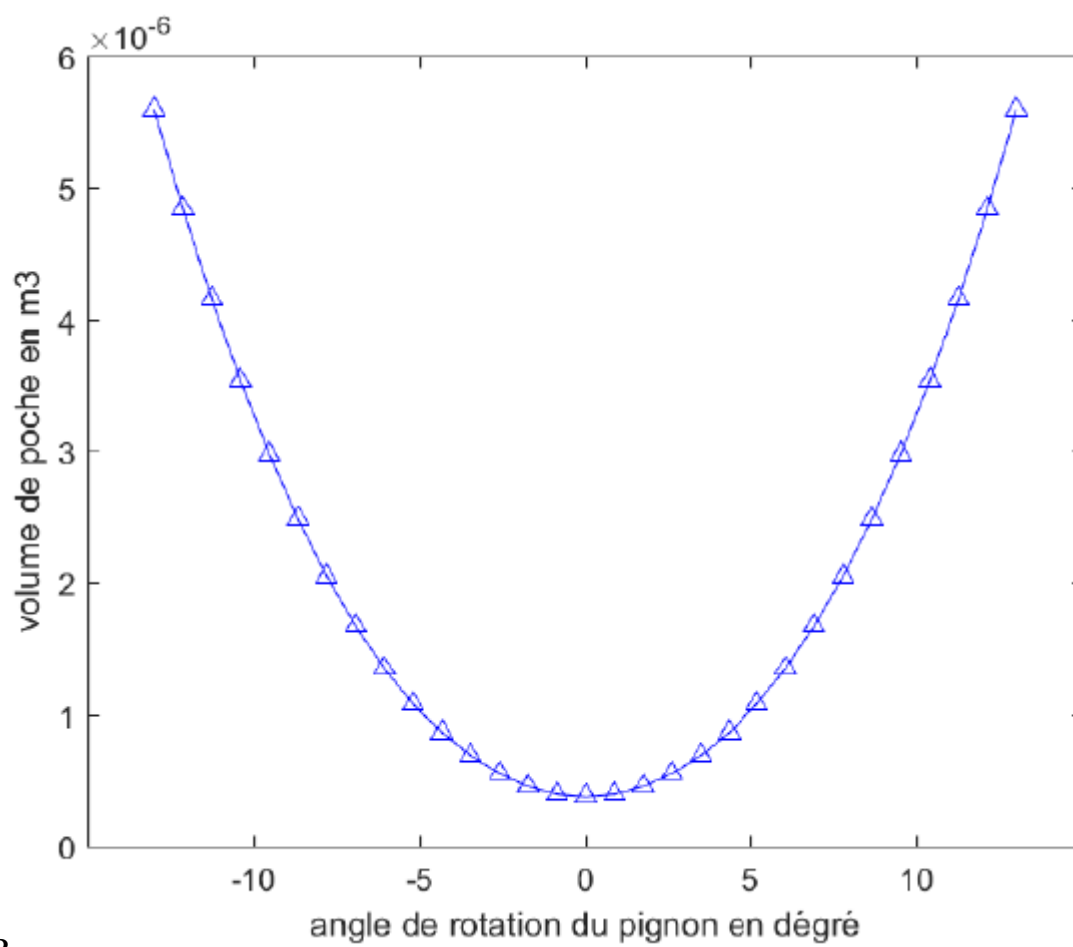
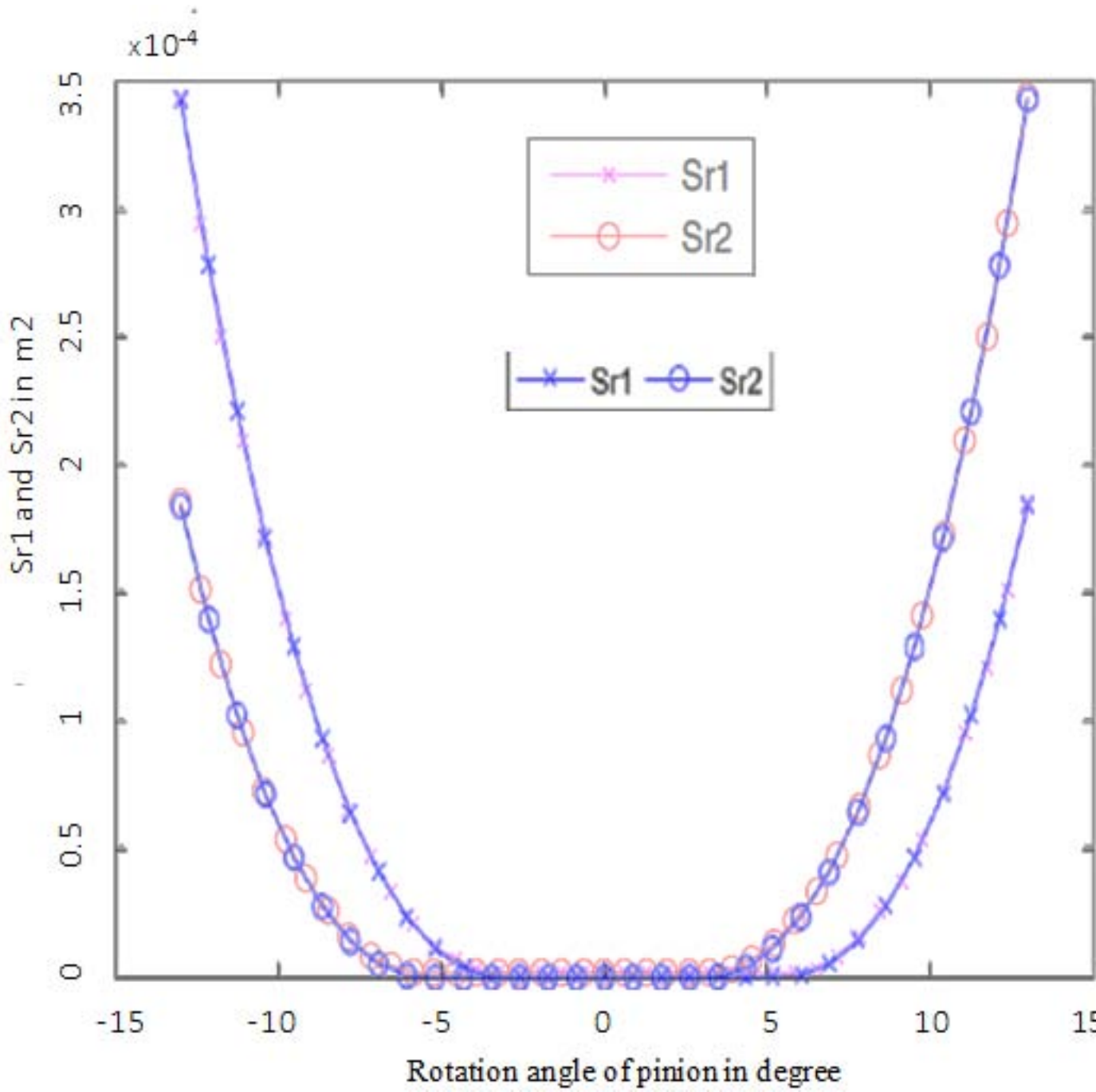


Figure 18:



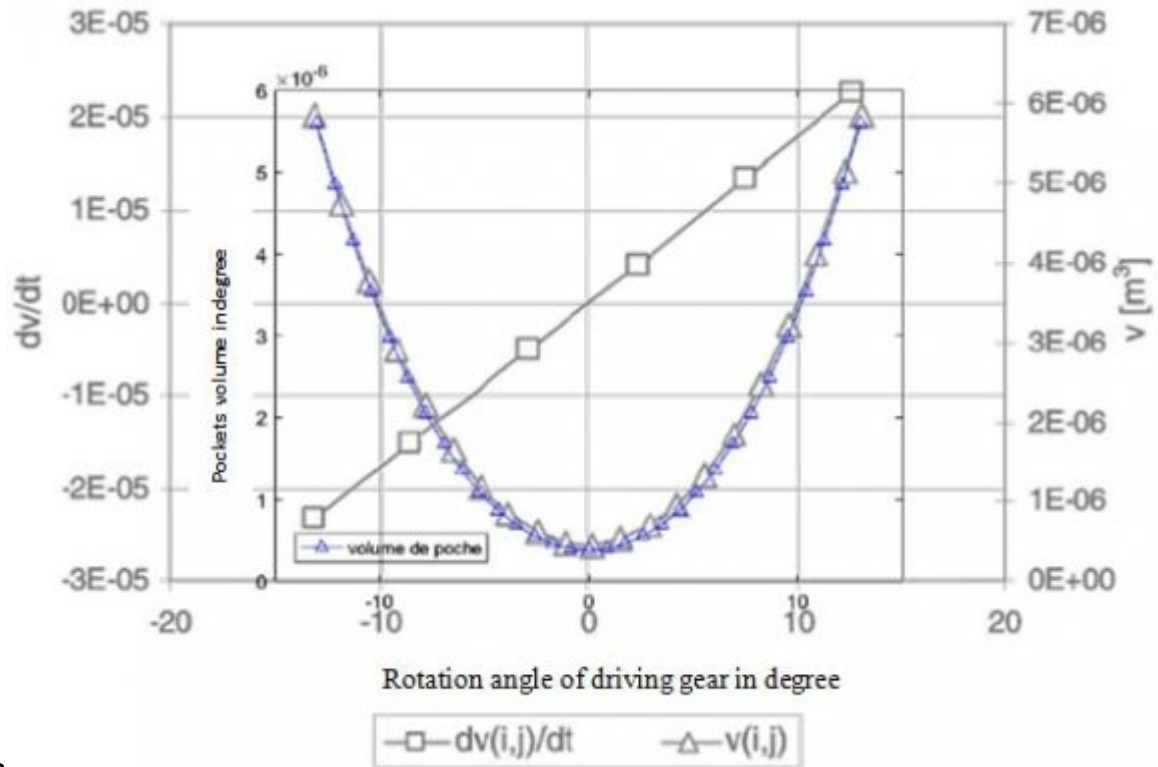
12

Figure 19: Figure 12 :



3

Figure 20: 3



13

Figure 21: Figure 13 :

1

Year 2022
 54
 II V ersion I
 (A) Volume Xx XII
 Issue
 Global Journal of
 Researches in Engi-
 neering

IV. Results By applying the equations (1) to (13), we obtain 03 types tooth profile: a)

Gear 2	40	10	20°-
			0.2
Gear 3	76	4	20°0

© 2022 Global Journals

Figure 22: Table 1 :

2

	Number teeth	of	m(module) ??(pressure angle)	x(shift coefficient)	b(mm)
pinion	76		4 20°0		100
gear	76		4 20°0		100

Figure 23: Table 2 :

- 344 [Maurer and]lastunabhängiger Zahnungsverlusteschnellaufender Stirnradgetriebe () , J Maurer ,]lastunab-
345 hängiger Zahnungsverlusteschnellaufender Stirnradgetriebe . 1994. Stuttgart. Universität Stuttgart
- 346 [Zhai et al.] *A Mathematical Model for Parametric Tooth Profile of Spur Gears*, Guodong Zhai , Zhihao Liang ,
347 Zihao Fu .
- 348 [Pechersky and Wittbrodt ()] ‘An Analysis of Fluid Flow Between Meshing Spur Gear Teeth’. M J Pechersky ,
349 M J Wittbrodt . *Proceedings of the ASME Fifth International Power Transmission and Gearing Conference*,
350 (the ASME Fifth International Power Transmission and Gearing Conference Chicago, IL) 1989. p. .
- 351 [Anderson et al.] *An Analytical Method To Predict Efficiency of Aircraft Gearboxes*, N E Anderson , S H Loewen-
352 thal , J D Black . <[http://ntrs.nasa.gov/archive/nasa/casi.ntrs.nasa.gov/19840017538_](http://ntrs.nasa.gov/archive/nasa/casi.ntrs.nasa.gov/19840017538_1984017538.pdf)
353 [1984017538.pdf](http://ntrs.nasa.gov/archive/nasa/casi.ntrs.nasa.gov/19840017538_1984017538.pdf)> (en ligne). NASA Technical Memorandum 83716, 1984. Disponible sur
- 354 [Devin and Hilty ()] ‘An experimental investigation of spin power losses of planetary gear sets’. R Devin , B S
355 Hilty . *Thesis for the degree Master of Science*, 2010. The Ohio State University
- 356 [Rohn and Handschuch] *Efficiency testing of a helicopter transmission planetary reduction stage*, D A Rohn ,
357 R F Handschuch . <[http://ntrs.nasa.gov/archive/nasa/casi.ntrs.nasa.gov/19880005842_](http://ntrs.nasa.gov/archive/nasa/casi.ntrs.nasa.gov/19880005842_1988005842.pdf)
358 [1988005842.pdf](http://ntrs.nasa.gov/archive/nasa/casi.ntrs.nasa.gov/19880005842_1988005842.pdf)> (en ligne). NASA Technical Paper 2795, 1988. Disponible sur
- 359 [Krantz] *Experimental and analytical evaluation of efficiency of helicopter planetary stage*, T L Krantz . <[http://](http://ntrs.nasa.gov/archive/nasa/casi.ntrs.nasa.gov/19910003643_1991003643.pdf)
360 ntrs.nasa.gov/archive/nasa/casi.ntrs.nasa.gov/19910003643_1991003643.pdf> (en
361 ligne). NASA Technical paper 3063, 1990. Disponible sur
- 362 [Diab et al. ()] ‘Experimental and Numerical Investigations on the Air-Pumping Phenomenon in High-Speed
363 Spur and Helical Gears’. Y Diab , F Ville , H Houjoh , P Sainsot , P Velex . *Proceedings of the Institute of*
364 *Mechanical Engineers* 2005. 219 p. .
- 365 [Faydor et al. ()] *Gear Geometry and Applied Theory*”, *SECOND EDITION*, Cambridge university press, L Faydor
366 , Alfonso Litvin , Fuentes . 2004.
- 367 [Spitas and Spitas] *Generating Interchangeable 20° Spur Gear Sets with Circular Fillets to Increase Load Carrying*
368 *Capacity*, Christos A Spitas , Vasilis A Spitas .
- 369 [Terekhov ()] ‘Hydraulic losses in gearboxes with oil immersion’. A S Terekhov . *Russ Eng J* 1975. 55 p. .
- 370 [Mauz ()] *Hydraulische Verluste von Stirnradgetriebe bei Umfangsgeschwindigkeit bis 60m/s*, W Mauz . 1987. IMK
371 University of Stuttgart (PhD Dissertation) (209 p.)
- 372 [Butsch ()] ‘Hydraulische Verlusteschnell-laufender Stirnradgetriebe’. M Butsch . *PhD Dissertation: IMK Univer-*
373 *sity of Stuttgart, 157 p*, 1989.
- 374 [Diab et al. ()] ‘Investigations on Power Losses in High Speed Gears’. Y Diab , F Ville , P Velex . *Part J: J. Eng.*
375 *Tribol* 2006. 220 p. . (Proc. Inst. Mech.Eng.)
- 376 [Seetharaman and Kahraman ()] ‘Load-independent spin power losses of a spur gear pair: Model formulation’. S
377 Seetharaman , A Kahraman . *Journal of Tribology* 2009. 131.
- 378 [Hindawi] *Mathematical Problems in Engineering*, Hindawi . 10.1155/2020/7869315. ID 7869315. <https://doi.org/10.1155/2020/7869315> 2020.
379
- 380 [Lasri et al. ()] ‘Pertes de puissance par piégeage de l’huile lubrifiant dans les engrenages” 13ème Congrès
381 de Mécanique 11 -14 Avril’. A Lasri , L Belfals , B Najji , M Zaoui . 10.1051/meca/2014046. [www.mechanics-](http://www.mechanics-industry.org)
382 [mechanics-industry.org](http://www.mechanics-industry.org) *EDP Sciences* 2017. 2014. (AFM)
- 383 [Lasri et al. ()] ‘Preliminary modeling of the oil trapping between teeth for spur gears’. Abdelilah Lasri , F Ville
384 , Lahcen Belfals , Brahim Najji . 10.1051/meca/2014046. www.mechanics-industry.org *Mechanics &*
385 *Industry* 2014. 2014. EDP Sciences. 15 p. .
- 386 [Lasri et al. ()] ‘Pressure Estimation of the Trapped and Squeezed Oil between Teeth Spaces of Spur Gears’.
387 Abdelilah Lasri , Lahcen Belfals , Brahim Najji , Bernard Mushirabwoba . 10.12988/ams.2014.47542.
388 <http://dx.doi.org/10.12988/ams.2014.47542> *HIKARI Ltd, www.m-hikari.com*, 2014. 8 p. .
- 389 [Marco Ceccarelli Editor ()] ‘Proceedings of EUCOMES 08’. Marco Ceccarelli Editor . *The Second European*
390 *Conference on Mechanism Science*, 2009. Springer Science+Business Media B.V.
- 391 [Colbourne ()] *The Geometry of Involute Gears*, J R Colbourne . 10.1007/978-1-4612-4764-7. 1987. Springer-
392 Verlag New York Inc.
- 393 [Rundo ()] ‘Theoretical flow rate in crescent pumps’. Massimo Rundo . www.elsevier.com/locate/simpat
394 *Simulation Modelling Practice and Theory* 2017. ELSEVIER. 71 p. .
- 395 [Talbot ()] *Theoretical investigation of the efficiency of planetary gear sets*, David C Talbot . 2012. (these de
396 Doctor at à l’université de l’Etat d’Ohio au USA)